Vitamin D rescues pancreatic β cell dysfunction due to iron overload via elevation of the vitamin D receptor and maintenance of Ca^{2+} homeostasis

Yoo Jeong Lee[a1], Gyu Hee Kim[a1], Jin-soo Yoo[b], Sang Ick Park[a], and Joo Hyun Lim[a*]

[a]Division of Endocrine and Metabolic Disease, Center for Biomedical Sciences, [b]Division of Bio-Medical Informatics, Center for Genome Science, Korea National Institute of Health, Cheongju, Chungbuk, 28159, Republic of Korea

[1] These authors equally contributed in this work.

*** Corresponding author**:

Joo Hyun Lim, PhD.

E-mail: mikorio@korea.kr, Telephone: +82-43-719-8691, Fax: +82-43-719-8602

Keywords: iron overload, pancreatic β cell failure, vitamin D, Ca^{2+} homeostasis

Abbreviations: $1,25(OH)_2D_3$: 1,25-dihydroxyvitamin D_3; $25(OH)D_3$: 25-hydroxyvitamin D_3; HAMP: Hepcidin antimicrobial peptide (Hepcidin); SLC8A1: Solute carrier family 8 member A1; SLC11A2: Solute carrier family 11 member 2; VDR: Vitamin D receptor

Received: 04/08/2020; Revised: 08/12/2020; Accepted: 09/12/2020

This article has been accepted for publication and undergone full peer review but has not been through the copyediting, typesetting, pagination and proofreading process, which may lead to differences between this version and the Version of Record. Please cite this article as doi: 10.1002/mnfr.202000772.

ABSTRACT

Scope: Accumulating evidence indicates that micronutrients are related to metabolic diseases. However, comparatively less attention has been devoted to their influence on each other during the development of metabolic diseases. To investigate the underlying mechanisms, we examined the effects of iron and vitamin D on pancreatic β cell functions.

Methods and results: We induced iron overload in INS-1 rat insulinoma pancreatic β cells and found that iron overload dramatically reduced expression of the vitamin D receptor (*VDR*). Iron overload-induced β cell dysfunction was rescued by $1,25(OH)_2D_3$ cotreatment via restoration of VDR level and the consequent maintenance of Ca^{2+} homeostasis. We also observed iron accumulation in the islets of 22-month-old C57BL/6 mice fed a chow diet (1,000 IU vitamin D_3/kg). In contrast, islet iron accumulation and hyperinsulinemia were ameliorated in mice fed a vitamin D_3-supplemented diet (20,000 IU/kg).

Conclusions: We showed that functional failure of β cells due to iron accumulation was rescued by $1,25(OH)_2D_3$, and iron overload significantly reduced VDR levels in β cells. These results suggest that iron and vitamin D inversely influence pancreatic β cell function.

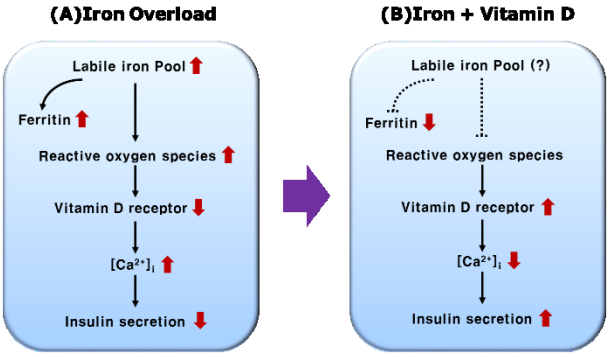

(A) Iron overload: abnormal elevation of ROS due to the accumulation of LIP reduces VDR, which subsequently disturbs Ca^{2+} homeostasis and insulin secretion. Also cellular ferritin accumulation is increased. (B) Vitamin D supplementation restores Ca^{2+} homeostasis via recovery of the VDR, and in turn GSIS in β cells. The accumulation of iron is reduced.

1. Introduction

Iron is an essential micronutrient that is involved in important biological mechanisms, such as erythropoiesis and systemic immune responses. In previous decades, an iron deficiency cause of diseases, such as anemia, was the primarily focus; however, excess iron is currently the focus as a high-risk factor for metabolic syndrome and cardiovascular diseases [1]. Because of the high reactivity and toxicity of iron, delicate mechanisms evolved to maintain iron homeostasis. Dietary iron is primarily absorbed into the duodenum via Solute carrier family 11 member 2 (*Slc11a2*) after reduction from ferric iron (Fe^{3+}) to ferrous iron (Fe^{2+}), and it is exported basolaterally via the iron exporter ferroportin. Hepcidin (*HAMP*) is the key iron regulatory hormone primarily expressed in liver, and it binds ferroportin under iron overload conditions, which triggers its degradation to regulate the amount of circulating iron. The iron released from ferroportin circulates as a form of diferric transferrin complex (Tf-Fe2). Cells expressing transferrin receptors (*Tfrc*) ultimately use iron via endocytosis [2]. Excess iron in the plasma and cytoplasm is stored in the ferritin protein complex, and elevation of serum ferritin generally indicates whole-body iron overload, which is currently considered a hallmark of metabolic diseases [3]. Iron overload is also accompanied by the deposition of excess iron in cells and tissues, including pancreatic β cells, liver and muscles, which results in the functional failure of β cells, nonalcoholic fatty liver disease, skeletal muscle atrophy and sarcopenia [4, 5]. Pancreatic β cells contain large amounts of Slc11a2 and ferritin but almost no ferroportin, which suggests that iron accumulates easily in these cells [6, 7]. Kulaksiz *et al*. previously suggested that iron metabolism and glucose metabolism were correlated [8]. Iron accumulation in pancreatic β cells also affects cell mass and disrupts β cell function. Several studies reported that high glucose levels caused an upregulation of ferritin heavy chain (*FTH)* and downregulation of *HAMP*, concomitant with a reduction in pancreatic

and duodenal homeobox-1 (*PDX1*) in pancreatic β cells [9]. In addition, Simcox J. and McClain D. described that that iron overload very likely plays a critical role in pancreatic β cell functions and diabetes [10]. However, the precise molecular mechanisms have not been revealed.

Vitamin D is one of the most important micronutrients involved in many biological functions, such as bone metabolism and immune responses. Without dietary intake, vitamin D may be nonenzymatically formed from 7-dehydrocholesterol in the skin via sunlight. The major circulating form of vitamin D is 25-hydroxyvitamin D_3 ($25(OH)D_3$), which is produced by hydroxylation at the C-25 position via cytochrome P 450-containing (CYP) 2R1 in the liver. The $25(OH)D_3$ is further converted to the active form of vitamin D_3, 1,25-dihydroxyvitamin D_3 ($1,25(OH)_2D_3$), in the kidney via the mitochondrial enzyme CYP27B1. $1,25(OH)_2D_3$ activates CYP24A1, which is a key enzyme that initiates $1,25(OH)_2D_3$ catabolism in the kidney and prevents hypervitaminosis D, causing vascular calcification. This process creates a negative feedback loop of $1,25(OH)_2D_3$ production in the maintenance of vitamin D homeostasis [11]. The biological activity of vitamin D is initiated by its binding to its receptor, the vitamin D receptor (VDR). VDR belongs to the nuclear receptor superfamily and generally forms a heterodimer with the retinoid X receptor (RXR). VDR subsequently binds to the vitamin D-responsive element (VDRE) in its target genes. VDR has multiple posttranslational modification sites, including phosphorylation, acetylation and ubiquitination, which directly influence its function [12]. For example, phosphorylation at serine 208 enhances $1,25(OH)_2D_3$-stimulated transcriptional activity of VDR [13], whereas phosphorylation at serine 51 decreases the transcriptional activity of VDR. The most important biological effects of $1,25(OH)_2D_3$ are the maintenance of Ca^{2+} homeostasis and preservation of the low resting Ca^{2+} level in cells. $1,25(OH)_2D_3$ increases the expression of

the plasma membrane Ca^{2+}-ATPase (*ATP2B*) and solute carrier family 8 member A (*SLC8A*) to exclude Ca^{2+} from cells. It also stimulates the expression of Ca^{2+}-binding proteins, such as calbindin 1 (*CALB1*) and parvalbumin (*Pvalb*), which act as endogenous Ca^{2+} buffers to reduce Ca^{2+} levels [14]. Cellular Ca^{2+} levels are closely related to redox signaling and the generation of reactive oxygen species (ROS). Elevation of Ca^{2+} levels promotes mitochondrial ROS generation, and an increase in ROS production influences Ca^{2+} channels, such as RyR, IP3R and ATP2B. Therefore, vitamin D_3 also plays an important role in maintaining low cellular ROS levels [15]. These roles of vitamin D_3 seem to be closely related, that vitamin D_3 deficiency causes many pathologies, such as Alzheimer's disease, hypertension and type 2 diabetes mellitus (T2D). Vitamin D_3 has gradually become a therapeutic target in T2D, and many groups studied the clinical benefits of vitamin D_3 supplementation on T2D [16]. Nevertheless, the main outcomes remain controversial. Vitamin D_3 improves insulin secretion from pancreatic β cells [17], and VDR gene polymorphisms are closely associated with diabetes [18, 19]. Knockout of VDRs in mice disrupted insulin secretion [20], and tissue-specific overexpression of *VDR* in pancreatic β cells prevented diabetes in mice [21].

We provide the first evidence that iron directly suppresses the VDR level and that $1,25(OH)_2D_3$ treatment rescues iron overload-induced pancreatic β cell dysfunction. Collectively, these findings suggest that the balance between iron and vitamin D_3 levels is important in preventing the development of T2D.

2. Experimental Section

2.1. Cell culture and reagent

The rat insulinoma cell line INS-1 was purchased from Addexbio (San Diego, CA, USA). Cells were maintained in RPMI-1640 medium (Gibco; Thermo Fisher Scientific, Inc., Waltham, MA, USA) supplemented with 1% penicillin-streptomycin (Gibco), 10% fetal bovine serum (FBS; Gibco), 50 μM β-mercaptoethanol, 2 mM L-glutamine, and 25 mM HEPES in 5% CO2 at 37 °C and passaged every 3-4 days. Cells were treated with 100, 150, or 200 μM Fe-NTA for 24 h or 48 h. Deferoxamine (DFO), N-acetylcysteine (NAC), 1α,25-dihydroxyvitamin D_3, nitrilotriacetic acid (NTA) and ferric nitrate were purchased from Sigma-Aldrich (St. Louis, MO, USA).

2.2. Animals and Dosage Information

Male C57BL/6 mice (6 and 18 months old, n = 10-12 per group) were obtained from the Animal Facility of Aging Science, Korea Basic Science Institute (KBSI) Gwangju Center (Gwangju, Korea) and housed at a constant room temperature (RT; 23 °C) on a 12-h light/dark cycle with free access to food and water. After one week of adaptation, 6- and 18-month-old mice were randomly assigned to two groups and fed for 4 months as follows: control group, fed a standard chow diet (AIN-93G, Research Diets, New Brunswick, NJ, USA) containing vitamin D_3 (1,000 IU per kg body weight); and a vitamin D_3 supplement group, fed a standard chow diet enriched with vitamin D_3 (20,000 IU per kg body weight). All animal procedures were performed according to the guidelines of the Korean National Institutes of Health Animal Care and Use Committee (permit number: KCDC-032-20-2A), and the mice were cared for in accordance with the Korea National Institute of Health guidelines.

2.3. Measurement of intracellular labile iron

Fe-NTA-treated or untreated INS-1 cells were incubated with 0.5 μM calcein-AM (Molecular Probes, Eugene, OR, CA, USA) for 24 h at 37 °C. The cells were washed with PBS, and calcein fluorescence was measured in a fluorescent plate reader (Molecular Device, San Jose, CA, USA) with a set excitation wavelength of 488 nm and an emission wavelength of 520 nm.

2.4. Western blot analysis

Whole-cell lysates were extracted in RIPA extraction buffer, and protein concentrations were determined using a BCA protein assay (Pierce; Thermo Fisher Scientific, Inc., Waltham, MA, USA). Cell lysates (30 μg) were mixed with 20 μl of SDS-PAGE sample buffer and loaded on 4-12% SDS-PAGE gels. Antibodies against β-actin (#8457), phospho-eIF2α (#3597), cleaved caspase 3 (#9664), Parp (#8542), and insulin (#8138) were purchased from Cell Signaling Technology (Beverly, MA, USA). Antibodies against ferritin heavy chain (MBP1-31944) were obtained from Novus Biological (Centennial, CO, USA). Antibodies against IP3R (ab5804) and phospho-RyR2 (S2808) (ab59225) were purchased from Abcam (Cambridge, UK). Antibodies against VDR (sc-13133), lamin A/C (sc-6215), and α-tubulin (sc-8035) were purchased from Santa Cruz Biotechnology (Dallas, TX, USA). Antibodies against phospho-VDR (Ser51) (PA5-39757), and Glut2 (720238) were obtained from Thermo Fisher Scientific (Waltham, MA, USA), and antibodies against RyR2 (MBS9600004) were purchased from MyBioSource (San Diego, CA, USA).

2.5. Chromatin immunoprecipitation assay

Chromatin immunoprecipitation (ChIP) assays were performed using a ChIP Assay Kit (Millipore, Darmstadt, Germany), following the manufacturer's protocol. Briefly, cells were

subjected to crosslinking with 1% formaldehyde at room temperature (RT) at 10 min and quenched with glycine to a final concentration of 0.125 M. The cell pellets were sonicated in SDS lysis buffer. The supernatants were incubated with VDR antibody or normal IgG (Santa Cruz, Dallas, TX, USA) at 4˚C overnight then with Protein A/G for 1 h, eluted and precipitated in ethanol. The DNA was analyzed using qPCR and the primer pair, forward (F), CCTGGAACAAGTCAAGGGCTA, and reverse (R), AAGGGCAAGACTGTTCACCGT.

2.6. Immunohistochemistry

Pancreatic tissues were immediately fixed in 10% neutral buffered formalin for 24 h and embedded in paraffin. The paraffin-embedded blocks were sectioned at a thickness of 5 μm, dried, deparaffinized, and washed. The sections were treated with diluted blocking serum for 30 min then incubated overnight at 4 °C with ferritin (Novus, Centennial, CO, USA) or VDR (Santa Cruz, Texas, USA) antibodies. The sections were washed and incubated with biotinylated anti-rabbit and anti-mouse antibodies (Vector Laboratories, Burlingame, CA, USA) for 1 h at RT and incubated with the ABC kit (Vector Laboratories, CA, USA) for 30 min at RT. Immunostaining was developed with DAB solution (D3939, Sigma, St. Louis, MO, USA) for 5 min. The tissue sections were counterstained with a hematoxylin solution (Sigma). Images of the whole slide were captured using an inverted microscope (Olympus, Japan) with the MetaVue software. Quantitative analysis of DAB staining was performed using ImageJ Fiji (WS Rasband, National Institute of Health, Bethesda, MD, USA).

2.7. Statistical analysis

All results are expressed as the means ± standard errors of the mean (SEMs). Statistical analyses were performed using GraphPad Prism software (GraphPad, San Diego, CA, USA). Comparisons between two groups were performed using Student's t-test or the nonparametric

Mann–Whitney U test. For multiple-group comparisons, one-way analysis of variance (ANOVA) with Tukey's post hoc test for multiple comparisons was used to evaluate significant differences. Values of $p < 0.05$ were considered statistically significant.

3. Results

3.1. Disruption of pancreatic β cell functions by iron overload

To examine the precise molecular mechanisms by which iron overload disrupts pancreatic β cell functions, we first established a cell model using INS-1 rat insulinoma pancreatic β cells. Cellular ferritin was accumulated with increasing iron concentrations. At the same time, Calcein fluorescence was drastically reduced, which is quenched by labile iron pool (LIP) (figure 1A). Accompanied by the increasing LIP, the cell viability was gradually reduced (figure 1B). Concomitantly, endoplasmic reticulum (ER) stress responses and apoptotic responses were triggered by long-term treatment with Fe-NTA, but declined by pretreatment of the iron chelator, DFO (figure 1C). We next assessed whether factors involved in iron homeostasis were altered. Hepcidin and iron regulatory protein (IRP) 1 and 2 are major regulatory proteins that maintain iron homeostasis. IRP1 and IRP2 are key intracellular iron regulators that bind to iron-responsive elements (IREs) in the 5′ or 3′-untranslated regions (UTRs) of target genes and posttranscriptionally regulate their expression [2]. For example, IRPs suppress the translation of *Tfrc* and *Slc11a2* but accelerate the translation of ferritin when the cellular iron level is high. The expression levels of *HAMP* and *Irp 1* and *2* gradually increased with prolonged iron accumulation in an effort to maintain iron homeostasis, thereby, the expression of *Tfrc* was decreased. However, the expression of *Slc11a2* was increased with continuous iron exposure (figure 1D). This finding is similar to Hansen J *et al*. who indicated that Slc11a2 was primarily responsible for iron-mediated pancreatic β cell failure induced by the proinflammatory cytokine interleukin 1β (IL-1β) [22]. To confirm whether iron overload disrupted INS-1 cell functions, we measured glucose-stimulated insulin secretion (GSIS) and insulin production. Treatment with 65 μM Fe-NTA significantly dysregulated GSIS (figure 2A), and prolonged iron overload reduced the levels of glucose

transporter 2 (Glut 2) and insulin, which were restored by the iron cheater, DFO. The nuclear localization of PDX-1 was also decreased (figure 2B). Correspondingly, the cellular ATP levels, on which insulin secretion is dependent, were drastically reduced with increasing iron concentrations and were restored by DFO (figure 2C). Mitochondria are the essential organelles for ATP production, and many mitochondrial oxidative phosphorylation (OXPHOS) complexes contain Fe/S clusters. Therefore, we evaluated mitochondrial function and found that iron overload diminished the mitochondrial membrane potential (figure 2D). Because of its high reactivity, labile iron easily disrupts cellular redox mechanisms and produces massive amounts of ROS [23]. Mitochondrial dysfunction is related to the abnormal generation of ROS [24]. We then measured the intracellular ROS levels and confirmed that iron overload specifically increased the ROS levels, and pretreatment with 150 μM DFO or NAC, an ROS scavenger, decreased ROS levels (figure 2E). To verify the effects of the iron overload-induced accumulation of ROS, we first measured the activity of aconitase, which is a major enzyme of the tricarboxylic acid cycle, because aconitase contains 4 Fe/S clusters and its activity is readily decreased by oxidative stress. As shown in figure 2F, iron overload significantly reduced aconitase activity. We examined whether the abnormal increase in ROS production induced by iron overload was the main contributor to the reduction in GSIS in our system. As expected, pretreatment with NAC significantly inhibited the iron overload-induced reduction in GSIS, similarly to the effects of DFO (figure 2G). This result was consistent with the previous observation of Backe *et al*. who showed the relationship between increased ROS production due to iron overload and insulin secretion [25].

3.2. Iron overload reduced the amount of VDR in pancreatic β cells

To further elucidate the precise molecular mechanisms of iron overload-induced β cell dysfunction, especially via abnormal ROS generation, we used Ingenuity Pathway Analysis

(IPA) to perform enrichment analysis of the direct and indirect relationships between iron and pancreatic β cell functions. Among the identified network analysis, we especially focused on the interaction network linking ROS and Ca^{2+} homeostasis because these proteins are the key factors that influence the insulin secretion. From these IPA, we found Callens *et al*. previous report, which found 30 overlapping genes among the 105 differentially expressed genes in HL60 human leukemia cells treated with an iron chelator or $1,25(OH)_2D_3$, and the expression of *VDR* was elevated in cells treated with the iron chelator [26]. Syed S *et al.* [27] and Smith E. M. *et al.* [28] independently showed that vitamin D_3 downregulated *HAMP*. Based on these results, we hypothesized that VDR had a connection to iron. To examine whether iron affects VDR levels, we measured VDR levels in INS-1 cells after Fe-NTA treatment. Increasing concentrations of iron significantly reduced the total amount of VDR, and pretreatment with an iron chelator specifically recovered this reduction (figure 3A). *VDR* expression is strongly induced by its ligand, $1,25(OH)_2D_3$ [11]. The reduction of VDR due to iron overload was completely abolished with cotreatment with $1,25(OH)_2D_3$, as expected (figure 3B), NAC rescued the reduction in VDR levels, which indicated that the abnormal elevation of the cellular ROS level due to iron overload was mainly responsible for the reduction in VDR levels (figure 3C). We examined whether iron overload also accelerates the degradation of VDRs and found that iron overload reduces *VDR* expression and promoted its degradation (figure 3D).

As VDR is a nuclear receptor that is targeted to the nucleus, we measured changes in the localization of VDRs with increasing Fe-NTA concentrations after 24 or 48 h of treatment. Most VDR levels decreased significantly with increasing concentrations of Fe-NTA (figure 3E). Notably, only the serine 51-phosphorylated form of VDR was found in the cytosolic fraction in cells subjected to long-term treatment with Fe-NTA, which indicated that

prolonged treatment with excess iron reduced most VDRs and only the inactive form of VDR remained.

To assess whether the excess iron-induced reduction of VDR only occurred in pancreatic β cells, we treated the NRK-52E rat kidney proximal tubular epithelial cell line and SK-Hep1 human hepatic cell lines with excess iron because the kidney and liver are the most important organs in the maintenance of whole body vitamin D homeostasis. Excess iron also specifically reduced VDR protein levels in the liver and kidney cells, which indicates that excess iron generally reduces VDRs (figure 3F).

3.3. Iron overload disrupted Ca^{2+} homeostasis by reducing VDR levels in pancreatic β cells

GSIS in pancreatic β cells is initiated by rapid synchronous Ca^{2+} oscillations in the cells. To reinstate the Ca^{2+} oscillations, the accumulated Ca^{2+} in the cells is promptly sequestered by CALB1, absorbed into organelles or pumped out into the extracellular space via SLC8A and ATP2B. Therefore, a low steady-state cytosolic Ca^{+2} concentration ($[Ca^{+2}]i$) could be maintained. $1,25(OH)_2D_3$ regulates numerous Ca^{2+} channels. Therefore, we examined changes in the components mediating the maintenance of Ca^{2+} homeostasis. Iron overload caused alterations in these factors, which collectively resulted in an abnormal elevation of steady-state $[Ca^{2+}]i$, and cotreatment with DFO or $1,25(OH)_2D_3$ reversed these alterations (figure 4A). Previous studies found that RyRs became "leaky" with phosphorylation at serine 2808, which resulted in impaired glucose utilization and β cell function [29, 30]. Consistent with these reports, the level of RyR was reduced, and the serine 2808-phosphorylated form of RyR was greatly increased by iron overload (figure 4B), which may contribute to the elevation of $[Ca^{2+}]i$. To confirm whether iron overload truly altered steady-state $[Ca^{2+}]i$, we

measured steady-state $[Ca^{2+}]i$ using the Ca^{2+}-sensitive fluorescent dye Fluo-8 AM. Fe-NTA significantly increased steady-state $[Ca^{2+}]i$ and cotreatment with $1,25(OH)_2D_3$ reduced this increase (figure 4C). In addition to the maintain low steady-state $[Ca^{2+}]i$, voltage-gated calcium channels (VGCCs) are important to evoke synchronized Ca^{2+} oscillation for GSIS. Kjalarsdottir L *et al.* previously reported that $1,25(OH)_2D_3$ enhanced GSIS via upregulation of *Cacna1e*, an R-type VGCC [31]. Accordingly, we determined whether excess iron changes *Cacna1e.* Iron overload reduced the level of *Cacna1e*, and cotreatment with $1,25(OH)_2D_3$ rescued this reduction, as expected. We also used ChIP and showed that this excess iron-induced downregulation of *Cacna1e* was due to a reduction in the direct binding of VDRs to the target gene. Consistent with the expression, $1,25(OH)_2D_3$ restored *Cacna1e* binding to VDR (figure 4D).

To determine whether the restoration of Ca^{2+} homeostasis via $1,25(OH)_2D_3$ restores pancreatic β cell function, we next measured GSIS after cotreatment with iron and $1,25(OH)_2D_3$. Treatment with $1,25(OH)_2D_3$ rescued the iron overload-induced reduction in GSIS a similar degree as treatment with NAC or DFO (figure 4E), which suggests that $1,25(OH)_2D_3$ alone sufficiently restores the pancreatic β cell function disrupted by iron overload. To confirm this result, we performed primary cell culture using pancreatic islets obtained from 12 week-old C57BL/6 mice. Similar to our results in the INS-1 cells, $1,25(OH)_2D_3$ also rescued the excess iron-induced disturbance of insulin secretion (figure 4F).

3.4. Vitamin D3 prevented excess iron accumulation in the pancreatic β cells of aged mice

The aging population is rapidly increasing worldwide, and aging is currently considered to be closely related to the development of T2D [32]. Gregg T. *et al*. previously reported that an age-associated decline in mitochondrial function was responsible for the reduction in pancreatic β cell function in elderly individuals [33]. Additionally, Zhang *et al*. showed that excess iron accumulated in the livers and kidneys of aged C57BL/6 mice, which dysregulated iron metabolism [34]. Thus, we examined whether aging-associated disruption of pancreatic β cell function was associated with the accumulation of iron in pancreatic β cells and whether vitamin D_3 treatment could overcome the impairment of β cell functions, as observed in our cell model systems. We first measured the pancreatic islet mass from young (10-month-old) and aged (22-month-old) C57BL/6 mice. Consistent with Gregg *et al*., the mass of pancreatic β cells and the fasting insulin levels were significantly increased in aged mice compared to young mice (figure 5A and B). Notably, when the aged mice were fed a vitamin D3-supplemented diet (20,000 IU/kg), fasting hyperinsulinemia and the abnormal expansion of the islet mass were significantly reduced. Consistent with previous works [33, 35], the fasting glucose level in aged mice remained low due to hyperinsulinemia (figure 5C). Vitamin D_3 supplementation increased serum vitamin D_3 levels in young and aged mice (figure 5D), but there was no difference in serum ferritin levels (figure 5E). In contrast, iron accumulation was significantly increased in the β cells of aged mice compared to young mice, despite the low serum ferritin levels. Notably, the accumulation of iron in the β cells of aged mice fed the vitamin D_3-supplemented diet was obviously reduced (figure 6A). Serum insulin levels were also reduced in aged mice fed a vitamin D_3-supplemented diet (figure 5B). To investigate whether excessive iron accumulation in the β cells of aged mice influenced VDR, as observed in our cell model, we measured VDR levels in islets using immunohistochemistry using an anti-VDR antibody. VDR level decreased proportionally to iron accumulation in aged mice fed the chow diet. In contrast, VDR level in aged mice fed the vitamin D_3-supplemented diet

remained similar to young mice (figure 6B). Consistent with the islet mass and serum insulin measurements, the effects of vitamin D_3 supplementation were more compelling in aged mice than young mice.

4. Discussion

The importance of the proper maintenance of micronutrients for a healthy life increased in recent decades. Accumulating evidence indicates that micronutrients, especially iron and vitamin D, are related to metabolic syndrome [4, 14]. However, these studies only addressed the effects of individual micronutrients, and the possibility that micronutrients influence each other was overlooked. The present study is the first to demonstrate that vitamin D_3 and iron inversely influences pancreatic β cell functions. We found that iron overload not only reduced *VDR* expression but also accelerated VDR protein degradation. Most of the existing VDRs were in an inactive form. The reduction of VDRs changed Ca^{2+} channel expression and activity of RyR, and concomitantly disturbed Ca^{2+} homeostasis and GSIS in β cells. In contrast, $1,25(OH)_2D_3$ restored Ca^{2+} homeostasis via recovery of the VDR level, and in turn GSIS in β cells, which may be a main mechanism of $1,25(OH)_2D_3$ amelioration of iron overload-induced metabolic syndrome.

Due to the rapid worldwide increase in the aging population, interest in age-associated diseases increased recently. Aging itself is the representative risk factor for metabolic syndrome, and the incidence of T2D and impaired glucose tolerance is significantly increased in aging humans [36]. We first showed that vitamin D_3 supplementation prevented hyperinsulinemia and abnormal islet expansion, which are generally observed in aged mice. Glucose intolerance and concomitant hyperinsulinemia and islet expansion are also typically observed in mice fed a high-fat diet. Obesity induces β-cell hyperplasia due to the increase in macrophagy infiltration into the islets [37]. Borges *et al*. also reported that vitamin D_3 deficiency and a high-fat diet worsened the expansion of the pancreas and accelerated the development of structural irregularities [38]. We presumed that β-cell hyperplasia in aged mice was due to the increase of inflammation in the islets, similar to mice fed a high-fat diet.

Vitamin D has anti-inflammatory effects [11]. Therefore, vitamin D_3 supplementation in aged mice seems to prevent islet hyperplasia by reducing inflammation in the islets. Notably, vitamin D_3 supplementation was especially effective in aged mice. This result is consistent with studies in humans. Pines *et al*. described that vitamin D_3 supplementation was more beneficial in aged people than younger people [39]. Although aging is the typical risk factor for metabolic syndrome, not everyone who ages develops metabolic syndrome and T2D. We hypothesize that vitamin D_3 insufficiency is an important risk factor that leads to the development of metabolic diseases in aged individuals.

There is no consensus on the appropriate vitamin D_3 concentration in mice and humans because it is affected by very diverse circumstances, such as sex, age, race, region and season. Vitamin D_3 supplement intervention studies in humans are very diverse in the race, age, diseases status, etc. Kennel K. *et al.*'s review [40] stated that an optimal vitamin D_3 concentration would be 25-80 ng/ml and 44% of women over 80 years are vitamin D deficient (severe deficiency <10 ng/ml, mild to moderate deficiency 10-24 ng/ml). Syed S. *et al.* reported that when serum 25(OH)D_3 was above 30 ng/ml, serum hepcidin levels were lower in children with inflammatory bowel disease [27], which supports our results that iron and vitamin D_3 are inversely related. Madar A. *et al.* [41] and Braithwaite V. *et al.* [42] reported that vitamin D_3 supplementation to middle-aged humans did not affect serum ferritin level. Serum ferritin levels were also not altered in our animal model regardless of age and vitamin D_3 supplementation. Therefore, we hypothesized that the accumulation of iron in the organ (at least in pancreas), but not the elevation of serum ferritin level, was more harmful for the induction of metabolic diseases. Vitamin D_3 supplementation ameliorated this accumulation and thereby seemed to prevent metabolic disease. Further studies are needed to clarify how iron and vitamin D are inversely related to the development of metabolic diseases in humans.

In conclusion, we demonstrated that vitamin D ameliorated the negative effects of iron overload on pancreatic β cell functions. Conversely, iron overload suppressed the positive effects of vitamin D on pancreatic β cell functions by reducing VDR levels and concomitantly disturbing Ca^{2+} homeostasis in pancreatic β cells. vitamin D_3 supplementation effectively prevented iron accumulation in the pancreatic β cells of aged mice.

ACKNOWLEDGMENTS

This study was supported by an intramural research grant from the Korea National Institute of Health (2020-NG-014-00).

CONFLICT OF INTEREST STATEMENT

The authors declare that they have no conflicts of interest.

AUTHORS' CONTRIBUTIONS

J.H.L designed the study and wrote the manuscript. Y.J.L. wrote parts of this manuscript and primarily performed experiments and analyzed the data. G.H.K. primarily performed experiments and analyzed the data. J-S.Y performed the IPA analysis. S.I.P. discussed the results and commented on the manuscript.

References

[1] Ganz, T., *Physiological reviews*, **2013**, *93*, 1721.

[2] Hentze, M. W., Muckenthaler, M. U., Galy, B., Camaschella, C., *Cell*, *2010*, *142*, 24.

[3] Jung, C. H., Lee, M. J., Hwang, J. Y., Jang, J. E., Leem, J., Park, J. Y., Lee, J., Kim, H. K., Lee, W. J., *PloS one*, **2013**, *8*, e75250.

[4] Fernández-Real, J. M., Manco, M., *The lancet. Diabetes & endocrinology*, **2014**, *2*, 513.

[5] Zhao, G., *Biological trace element research*, **2018**, *186*, 379.

[6] Koch, R. O., Zoller, H., Theuri, I., Obrist, P., Egg, G., Strohmayer, W., Vogel, W., Weiss, G., *Histology and histopathology*, **2003**, *18*, 1095.

[7] Hudson, D. M., Curtis, S. B., Smith, V. C., Griffiths, T. A., Wong, A. Y., Scudamore, C. H., Buchan, A. M., MacGillivray, R. T., *American journal of physiology. Gastrointestinal and liver physiology*, **2010**, *298*, G425.

[8] Kulaksiz, H., Fein, E., Redecker, P., Stremmel, W., Adler, G., Cetin, Y., *The Journal of endocrinology*, **2008**, *197*, 241.

[9] Mao, X., Chen, H., Tang, J., Wang, L., Shu, T., *Endocrine connections*, **2017**, *6*, 121.

[10] Simcox, J. A., McClain, D. A., *Cell metabolism*, **2013**, *17*, 329.

[11] Gil, Á., Plaza-Diaz, J., Mesa, M. D., *Annals of nutrition & metabolism*, **2018**, *72*, 87.

[12] Zenata, O., Vrzal, R., *Oncotarget*, **2017**, *8*, 35390.

[13] Arriagada, G., Paredes, R., Olate, J., van Wijnen, A., Lian, J. B., Stein, G. S., Stein, J. L., Onate, S., Montecino, M., *The Journal of steroid biochemistry and molecular biology*, **2007**, *103*, 425.

[14] Berridge, M. J., *Biochemical journal*, **2017**, *474*, 1321.

[15] Berridge, M. J., *Philosophical transactions of the Royal Society of London. Series B, Biological sciences*, **2016**, 371.

[16] Muñoz-Garach, A., García-Fontana, B., Muñoz-Torres, M., *Nutrients*, **2019**, 11.

[17] Sergeev, I. N., *Hormone molecular biology and clinical investigation*, **2016**, *26*, 61.

[18] Bid, H. K., Konwar, R., Aggarwal, C. G., Gautam, S., Saxena, M., Nayak, V. L., Banerjee, M., *Indian journal of medical sciences*, **2009**, *63*, 187.

[19] Mukhtar, M., Batool, A., Wajid, A., Qayyum, I., *International journal of genomics*, **2017**, *2017*, 4171254.

[20] Zeitz, U., Weber, K., Soegiarto, D. W., Wolf, E., Balling, R., Erben, R. G., *Faseb j*, **2003**, *17*, 509.

[21] Morró, M., Vilà, L., Franckhauser, S., Mallol, C., Elias, G., Ferré, T., Molas, M., Casana, E., Rodó, J., Pujol, A., Téllez, N., Bosch, F., Casellas, A., *Diabetes*, **2020**, 69, 927.

[22] Hansen, J. B., Tonnesen, M. F., Madsen, A. N., Hagedorn, P. H., Friberg, J., Grunnet, L. G., Heller, R. S., Nielsen, A., Størling, J., Baeyens, L., Anker-Kitai, L., Qvortrup, K., Bouwens, L., Efrat, S., Aalund, M., Andrews, N. C., Billestrup, N., Karlsen, A. E., Holst, B., Pociot, F., Mandrup-Poulsen, T., *Cell metabolism*, **2012**, *16*, 449.

[23] Galaris, D., Barbouti, A., Pantopoulos, K., Biochimica et biophysica acta. *Molecular cell research*, **2019**, *1866*, 118535.

[24] Chen, T., Zhu, J., Wang, Y. H., Hang, C. H., *Neuroscience*, **2019**, *416*, 268.

[25] Backe, M. B., Moen, I. W., Ellervik, C., Hansen, J. B., Mandrup-Poulsen, T., *Annual review of nutrition*, **2016**, *36*, 241.

[26] Callens, C., Coulon, S., Naudin, J., Radford-Weiss, I., Boissel, N., Raffoux, E., Wang, P. H., Agarwal, S., Tamouza, H., Paubelle, E., Asnafi, V., Ribeil, J. A., Dessen, P., Canioni, D., Chandesris, O., Rubio, M. T., Beaumont, C., Benhamou, M., Dombret, H., Macintyre, E., Monteiro, R. C., Moura, I. C., Hermine, O., *The Journal of experimental medicine*, **2010**, *207*, 731.

[27] Syed, S., Michalski, E. S., Tangpricha, V., Chesdachai, S., Kumar, A., Prince, J., Ziegler, T. R., Suchdev, P. S., Kugathasan, S., *Inflammatory bowel diseases*, **2017**, *23*, 1650.

[28] Smith, E. M., Alvarez, J. A., Kearns, M. D., Hao, L., Sloan, J. H., Konrad, R. J., Ziegler, T. R., Zughaier, S. M., Tangpricha, V., *Clinical nutrition (Edinburgh, Scotland)*, **2017**, *36*, 980.

[29] Santulli, G., Pagano, G., Sardu, C., Xie, W., Reiken, S., D'Ascia, S. L., Cannone, M., Marziliano, N., Trimarco, B., Guise, T. A., Lacampagne, A., Marks, A. R., *The Journal of clinical investigation*, **2015**, *125*, 1968.

[30] Wehrens, X. H., Lehnart, S. E., Reiken, S. R., Marks, A. R., *Circulation research*, **2004**, *94*, e61.

[31] Kjalarsdottir, L., Tersey, S. A., Vishwanath, M., Chuang, J. C., Posner, B. A., Mirmira, R. G., Repa, J. J., *Journal of steroid biochemistry and molecular biology*, **2019**, *185*, 17.

[32] Centers for Disease Control and Prevention. *National Diabetes Statistics Report*, **2014**.

[33] Gregg, T., Poudel, C., Schmidt, B. A., Dhillon, R. S., Sdao, S. M., Truchan, N. A., Baar, E. L., Fernandez, L. A., Denu, J. M., Eliceiri, K. W., Rogers, J. D., Kimple, M. E., Lamming, D. W., Merrins, M. J., *Diabetes*, **2016**, *65*, 2700.

[34] Zhang, M. W., Zhao, P., Yung, W. H., Sheng, Y., Ke, Y., Qian, Z. M., *Aging*, **2018**, *10*, 3834.

[35] Cho, J. H., Lee, K. M., Lee, Y. I., Nam, H. G., Jeon, W. B., *Islets*, **2019**, *11*, 33.

[36] Kushner, J. A., *Journal of clinical investigation*, **2013**, *123*, 990.

[37] Ying, W., Fu, W., Lee, Y. S., Olefsky, J. M., *Nature reviews. Endocrinology*, **2020**, *16*, 81.

[38] Borges, C. C., Salles, A. F., Bringhenti, I., Souza-Mello, V., Mandarim-de-Lacerda, C. A., Aguila, M. B., *Molecular nutrition & food research*, **2016**, *60*, 346.

[39] Pines, A., *Climacteric : the journal of the International Menopause Society*, **2014**, *17*, 657.

[40] Kennel, K. A., Drake, M. T., Hurley, D. L., *Mayo Clinic proceedings*, **2010**, *85*, 752.

[41] Madar, A. A., Stene, L. C., Meyer, H. E., Brekke, M., Lagerløv, P., Knutsen, K. V., *Nutrition journal*, **2016**, *15*, 74.

[42] Braithwaite, V. S., Crozier, S. R., D'Angelo, S., Prentice, A., Cooper, C., Harvey, N. C., Jones, K. S., *Nutrients*, **2019**, *11*.

[43] Stull, N. D., Breite, A., McCarthy, R., Tersey, S. A., Mirmira, R. G., *Journal of visualized experiments : JoVE*, **2012**.

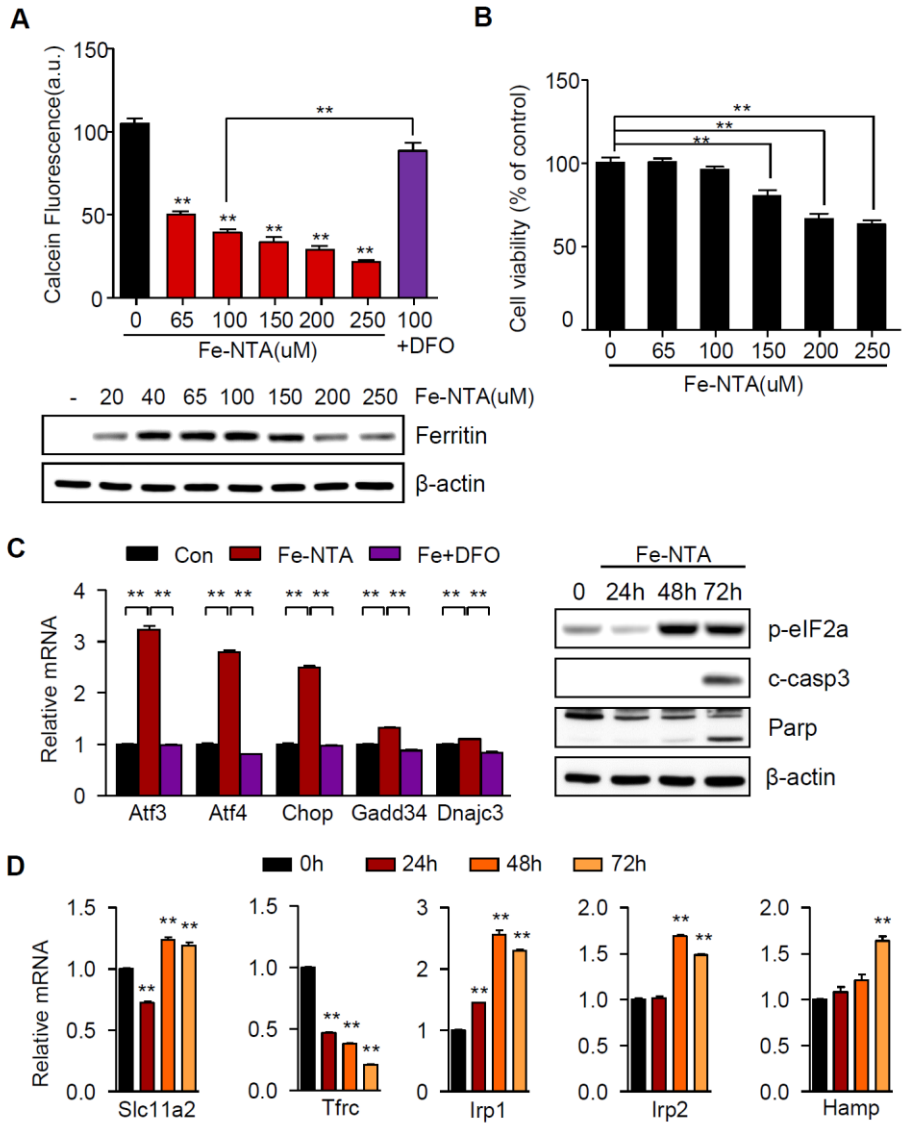

Figure 1. Induction of iron overload in pancreatic β cells. (A) Measurement of the LIP. INS-1 cells were incubated with calcein-AM after Fe-NTA treatment in the presence or absence of DFO for 24 h (n=8) (upper panel). Ferritin protein levels were determined after 24-h treatment with Fe-TNA as indicated (lower panel). (B) Cell viability was assessed using an MTT assay and is expressed as the percentage of control cell viability (n=8) (upper panel). Evaluation of ER stress responses using Western blot analysis (lower panel). (C) Cells were treated with 150 μM Fe-NTA for 48 h in the presence or absence of 200 μM DFO. Quantitative real-time PCR analysis of ER stress-related genes in cells. (D) Changes in the mRNA levels of genes related to iron homeostasis in Fe-NTA-treated cells at the indicated time points. All results are representative of more than three independent experiments. The data are presented as the means ± SEM values. Statistical analyses were performed using one-way ANOVA with Tukey's post hoc test for multiple comparisons. *p<0.05, **p<0.01.

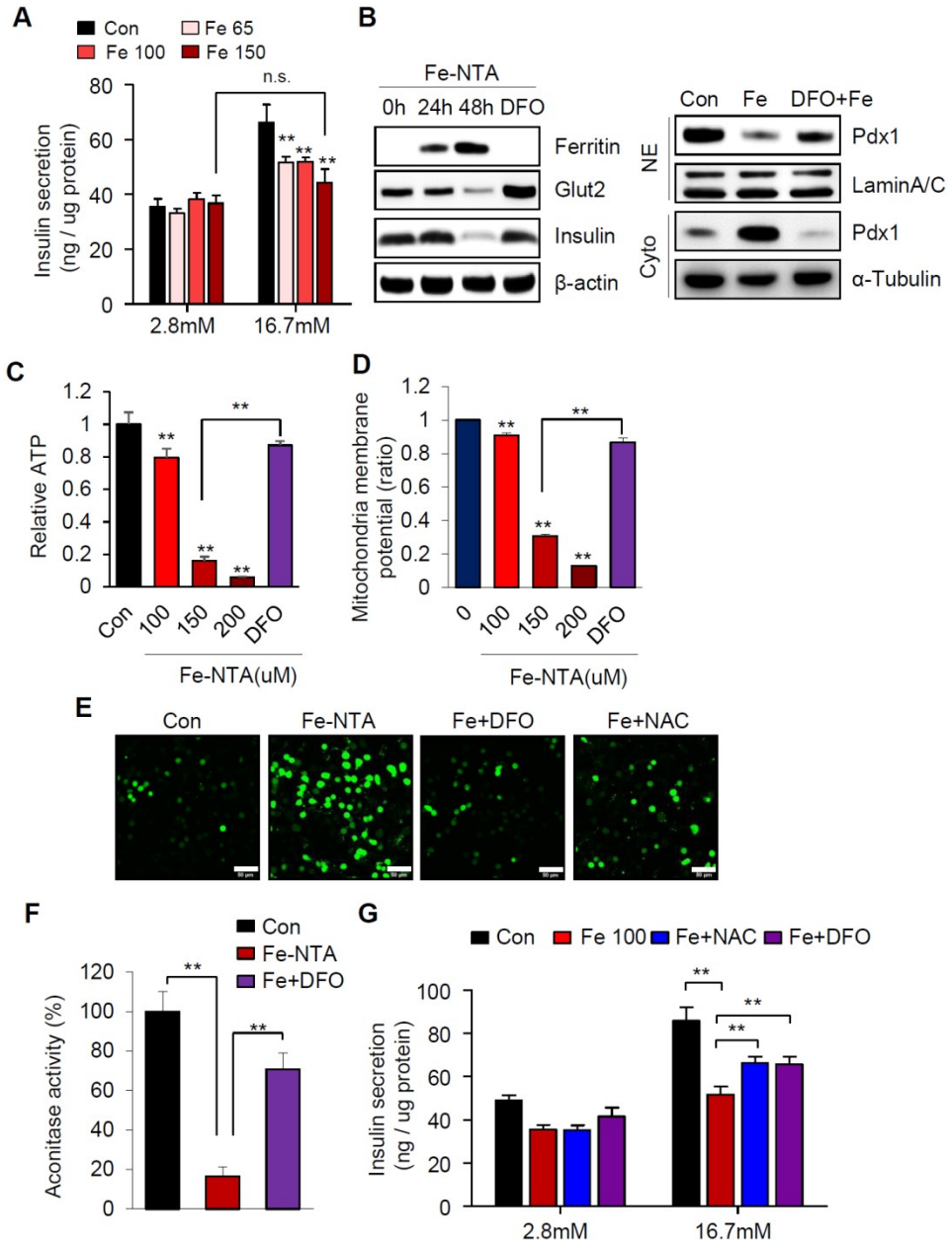

Figure 2. Disruption of β cell function by iron overload. (A) INS-1 cells were incubated with 2.8 mM or 16.7 mM glucose for 1 h, and insulin secretion was measured using an ELISA kit according to the manufacturer's instructions. Each value was normalized to the protein concentration. (B) Cells were treated with 150 μM Fe-NTA or 200 μM DFO as indicated. Protein levels of ferritin, Glut2, and insulin (upper panel) were measured. The nuclear fraction was isolated after treatment with Fe-NTA, and the amount of PDX-1 was determined

using Western blot analysis (lower panel). The intracellular ATP level (C) and mitochondrial membrane potential (D) were measured using an ATP assay kit and JC-1 assay kit, respectively, according to the manufacturer's instructions. (E) ROS levels in INS-1 cells treated with 150 μM Fe-NTA in the presence or absence of 200 μM DFO or 200 μM NAC. Scale bars = 50 μm. (F) Aconitase activity was measured using an aconitase activity assay kit. (G). Measurement of insulin secretion in INS-1 cells after exposure to 2.8 mM or 16.7 mM glucose. All results are representative of more than three independent experiments. The data are presented as the means ± SEM values. Statistical analyses were performed using one-way ANOVA with Tukey's post hoc test for multiple comparisons. *$p<0.05$, **$p<0.01$.

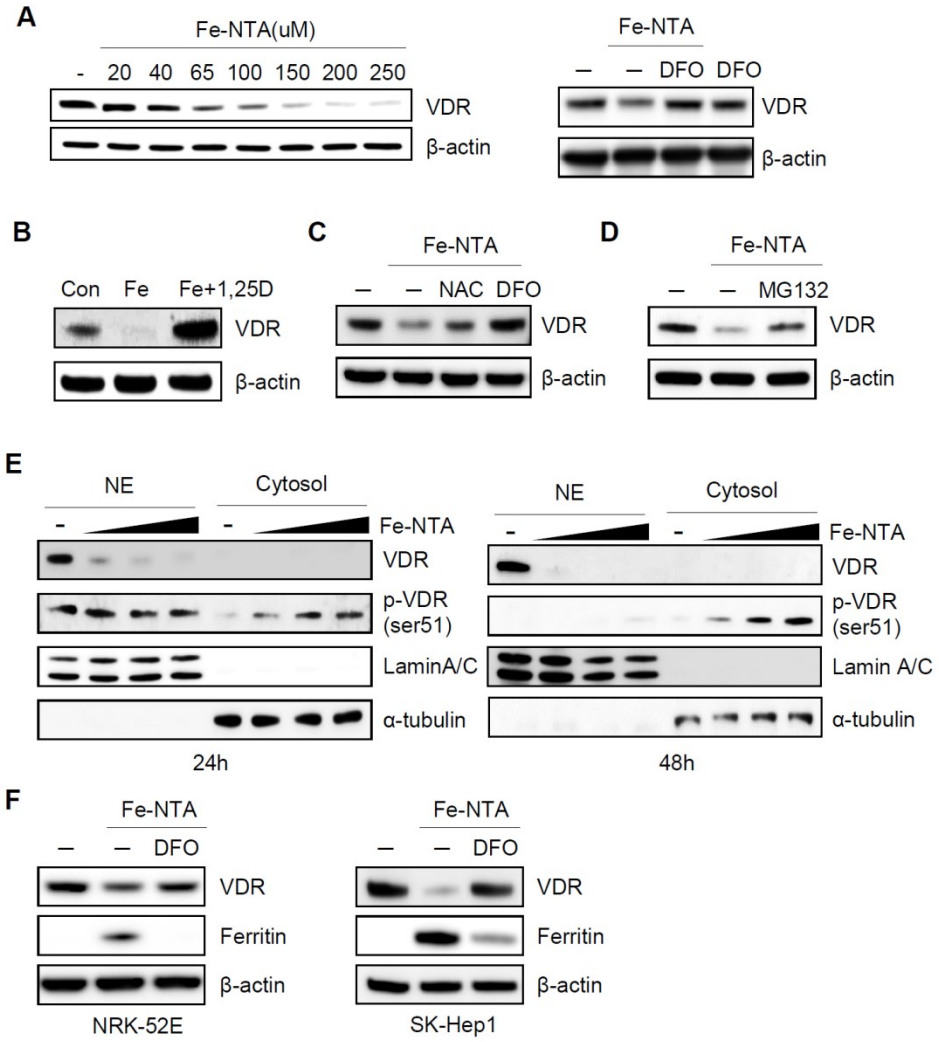

Figure 3. Reduction in the VDR level by iron overload. (A) INS-1 cells were treated with Fe-TNA for 24 h, as indicated. Analysis of the effect of Fe-NTA on the VDR level. (B) Changes in the levels of VDR in Fe-NTA-treated cells with or without 20nM $1,25(OH)_2D_3$ supplementation. (C) VDR levels in cells in the presence or absence of DFO or NAC. (D) The level of VDR was measured using Western blotting after treatment with 5 μM MG132 for 3 h. (E) INS-1 cells were treated with Fe-NTA (100, 150, 200 μM) for 24 h or 48 h then subjected to subcellular fractionation. Each fraction was analyzed using Western blotting with the indicated antibodies. (F) Changes in VDR and ferritin in NRK-52E and SK-Hep1 cells treated with Fe-NTA in the presence or absence of DFO. All results are representative of more than three independent experiments. The data are presented as the means ± SEM values. Statistical analyses were performed using one-way ANOVA with Tukey's post hoc test for multiple comparisons. *$p<0.05$, **$p<0.01$.

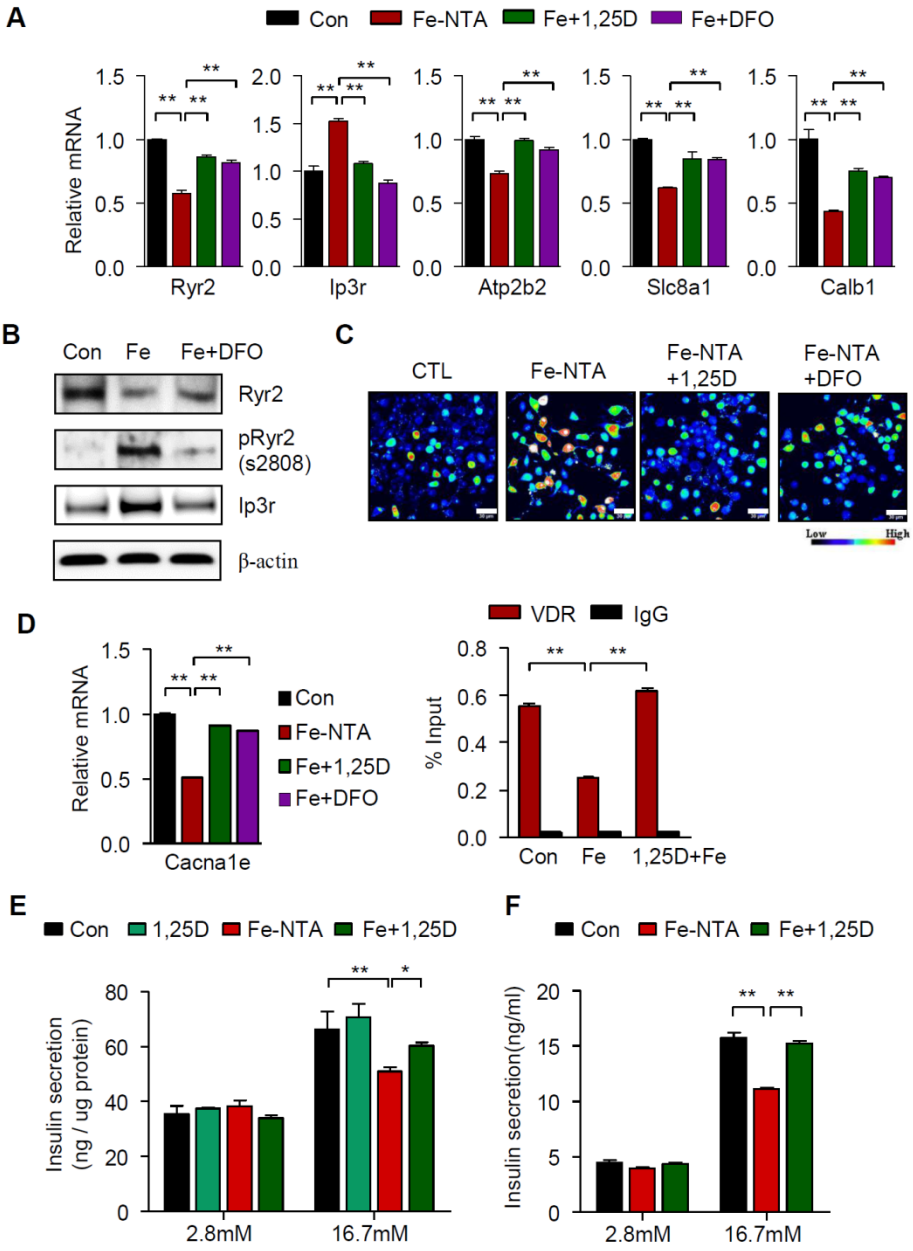

Figure 4. Restoration of Ca^{2+} homeostasis by $1,25(OH)_2D_3$ supplementation. (A) Quantitative real-time PCR analysis of *RyR2*, *Ip3r*, *Calb1*, *Atp2b2*, and *Slc8a1*. Cells were harvested in the presence or absence of DFO or VitD. (B) Immunoblot analyses of RyR2, phospho-RyR2 (Ser2808), and IP3R. (C) Measurement of the intracellular Ca^{2+} level in INS-1 cells after treatment with or without 20nM $1,25(OH)_2D_3$. Scale bars = 50 μm. Representative fluorescence imaging of cytosolic Ca^{2+} changes was performed using Fluo-8

AM. (D) ChIP followed by qPCR for VDR binding to the *Cacna1e* gene in cells treated with Fe-NTA in the presence or absence of $1,25(OH)_2D_3$. (E) INS-1 cells and (F) primary isolated mice [43] were incubated in the presence or absence of 20 nM $1,25(OH)_2D_3$ for 24 h, and insulin secretion was measured after exposure to 2.8 mM or 16.7 mM glucose. All results are representative of more than three independent experiments. The data are presented as the means ± SEM values. Statistical analyses were performed using one-way ANOVA with Tukey's post hoc test for multiple comparisons. *$p<0.05$, **$p<0.01$.

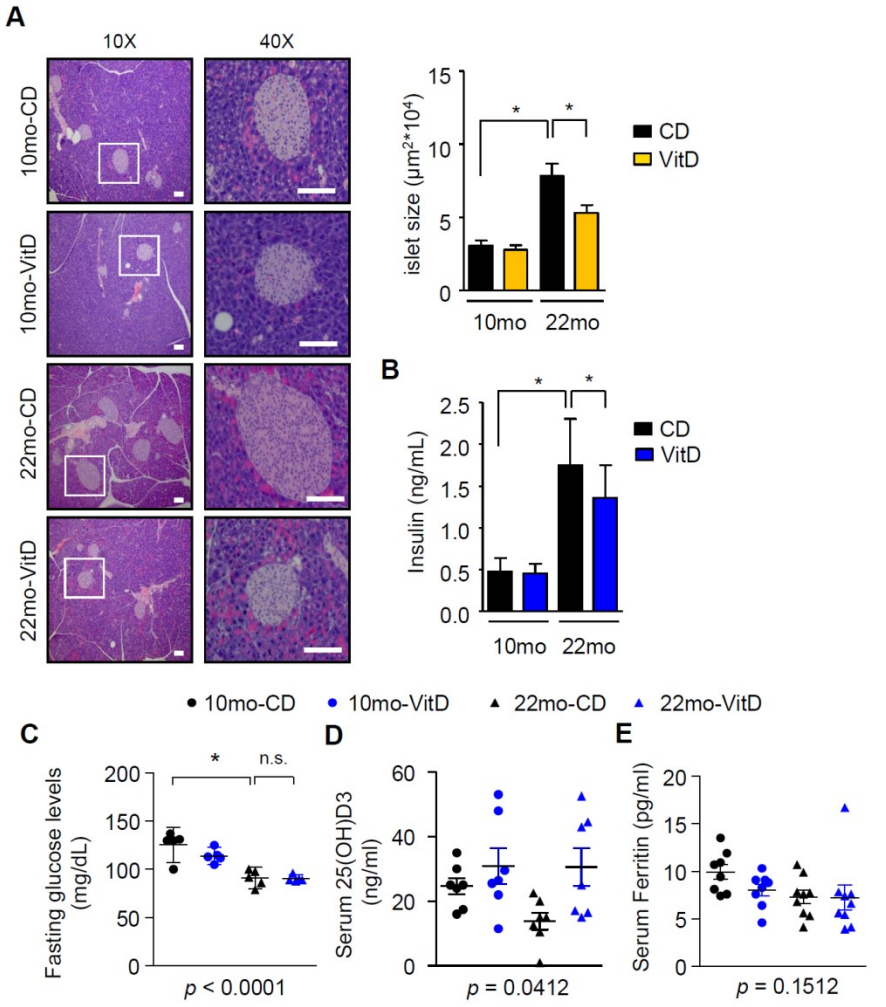

Figure 5. Prevention of β cell hyperplasia and hyperinsulinemia in aged mice by vitamin D_3 supplementation. (A) Representative images of H&E staining in pancreas tissue sections from mice at 10 or 22 months old (left); scale bar, 30 μm. Mean islet area of pancreatic sections (right). (B) Plasma insulin levels (EZRMI-13K Rat/Mouse Insulin ELISA kit, Millipore, Billerica, MA, USA), (C) short-term fasting (4 h) blood glucose levels (n=5), (D) serum 25(OH)D_3 levels (n=7) (ab213966 25-OH Vitamin D ELISA kit, Abcam, Cambridge, UK), and (E) serum ferritin levels (n=8-9) (ab157713 Ferritin mouse ELISA kit, Abcam, Cambridge, UK) were measured in 10-month-old and 22-month-old mice fed a control diet (CD) or a vitamin D_3-supplemented diet (VitD). All results are representative of more than three independent experiments. The data are presented as the means ± SEM values. Statistical analyses were performed using one-way ANOVA with Tukey's post hoc test for multiple comparisons. *p<0.05, **p<0.01.

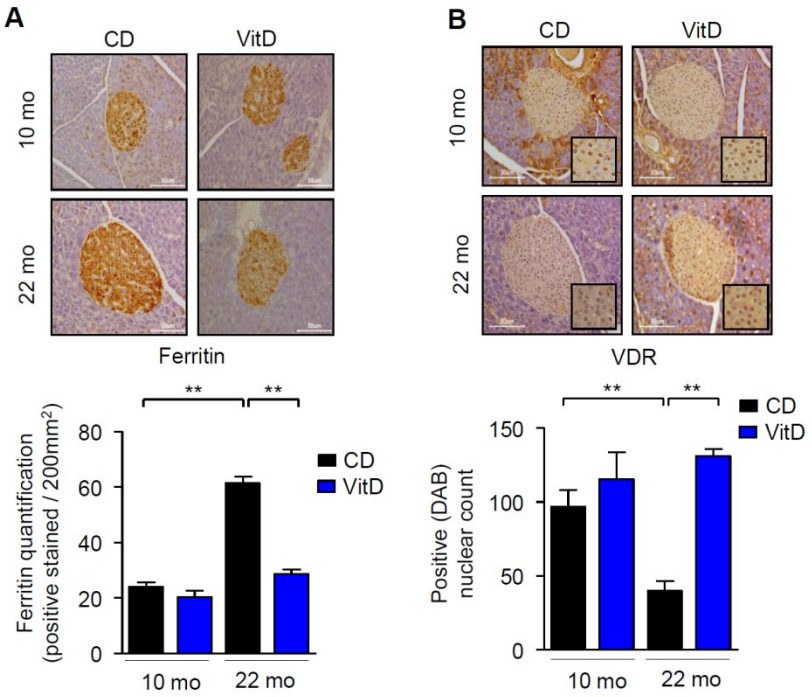

Figure 6. Prevention of iron accumulation in β cells of aged mice by vitamin D_3 supplementation. (A) Ferritin and (B) VDR levels were evaluated using immunohistochemistry as indicated. Scale bars = 30 μm. All results are representative of more than three independent experiments. The data are presented as the means ± SEM values. Statistical analyses were performed using one-way ANOVA with Tukey's post hoc test for multiple comparisons. *$p<0.05$, **$p<0.01$.